

Highly Imbalanced Regression with Tabular Data in SEP and Other Applications

Josias K. Moukpe*, Philip K. Chan*, Ming Zhang†

*Department of Electrical Engineering and Computer Science

†Department of Aerospace, Physics and Space Sciences

Florida Institute of Technology, Melbourne, FL, USA

jmoukpe2016@my.fit.edu, {pkc, mzhang}@fit.edu

Abstract—We investigate imbalanced regression with tabular data that have an imbalance ratio larger than 1,000 ("highly imbalanced"). Accurately estimating the target values of rare instances is important in applications such as forecasting the intensity of rare harmful Solar Energetic Particle (SEP) events. For regression, the MSE loss does not consider the correlation between predicted and actual values. Typical inverse importance functions allow only convex functions. Uniform sampling might yield mini-batches that do not have rare instances. We propose CISIR that incorporates correlation, Monotonically Decreasing Involution (MDI) importance, and stratified sampling. Based on five datasets, our experimental results indicate that CISIR can achieve lower error and higher correlation than some recent methods. Also, adding our correlation component to other recent methods can improve their performance. Lastly, MDI importance can outperform other importance functions. Our code can be found in <https://github.com/Machine-Earning/CISIR>.

Index Terms—regression, tabular, highly imbalanced, SEP

I. INTRODUCTION

Recent work on imbalanced regression usually focuses on images [6], [9], [17], [23], [25]. In this study, we investigate imbalanced regression with tabular data that have an imbalance ratio larger than 1,000 ("highly imbalanced"). We investigate methods without substantive additional computation due to factors such as additional synthetic data and pre-training for representation learning.

Accurately estimating the target values for rare instances is important in various applications. For example, forecasting the intensity of rare Solar Energetic Particle (SEP) [15] events helps provide warnings to alert astronauts to seek shelter and protect sensitive equipment. In this study, one SEP application is to forecast the future proton intensity based on features from electron intensity [14] and Coronal Mass Ejections (CMEs). Another is to forecast the peak proton intensity based on features from CMEs [18]. Three other applications are large torque values for a robot arm, high popularity in online news, and large amounts of feedback for blogs.

For regression, the typical loss function used for training a neural network model is the Mean Squared Error (MSE) between the model predictions and the actual target labels. However, MSE does not consider the correlation between predicted values and actual values. Consider evaluating 3 models on 5 instances in Figure 1. Model 1 (red) and Model 2 (green) have the same MSE of 2. According to MSE, Model

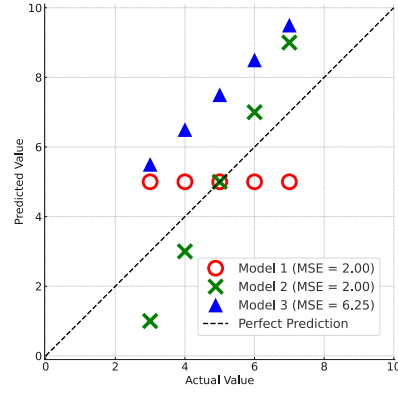


Fig. 1: An issue with MSE.

1 and Model 2 are equally inaccurate. However, the (same) predicted values of Model 1 are not correlated with the actual values, while the predicted values of Model 2 are positively correlated with the actual values. The predicted values should be positively correlated with the actual values, similar to the perfect reference (dotted black). Also, perfect MSE yields perfect positive correlation, while perfect positive correlation does not guarantee perfect MSE. For example, Model 3 (blue) in Figure 1 has a perfect positive correlation but a larger MSE than the other two models. Hence, while MSE alone is not sufficient, correlation alone is also not sufficient. Particularly, for rare and important instances in the real world (e.g. harmful SEP events), when the predicted values are increasing, we would like the actual values to be increasing correspondingly, which implies positive correlation. Otherwise, without correlation, the actual value might be increasing or decreasing, which implies more uncertainty. Hence, for imbalanced regression, we propose a weighted version of Pearson Correlation Coefficient (wPCC) to supplement the weighted MSE.

To handle imbalanced regression, one method is to weight rarer instances more in the loss function. Based on the probability density, the weight for each instance is governed by what we call an "importance function." We use "importance" to distinguish it from a "weight" in the model. One typical importance function is the inverse function [25] that aims to achieve a balanced distribution. DenseLoss [20] uses a linear function. Generally, we do not know the appropriate importance

function for an application because it is dependent on the dataset, imbalance ratio, and loss function. Hence, we propose Monotonically Decreasing Involution (MDI) importance, which allows a family of convex, linear, and concave functions. Also, MDI importance preserves the involution property exhibited by the inverse function that achieves the balanced distribution.

For highly imbalanced datasets, some of the mini-batches used in stochastic gradient descent (SGD) via uniform random sampling might not have any rare instances. That is, for some model updates, the gradient does not consider rare instances. To ensure rare instances are represented in each mini-batch, we propose stratified sampling for the mini-batches.

Our overall approach is called CISIR (Correlation, Involution importance, and Stratified sampling for Imbalanced Regression). Our contributions include:

- proposing weighted Pearson Correlation Coefficient (wPCC) as a secondary loss function,
- introducing MDI importance that allows convex, linear, and concave functions,
- stratified sampling in mini-batches to represent rare instances in each mini-batch,
- CISIR can achieve lower error and higher correlation than other recent methods,
- adding wPCC to other methods is beneficial in not only increasing correlation, but also reducing error, and
- MDI importance can outperform other importance functions.

II. RELATED WORK

Recent methods for imbalanced regression can be clustered into four groups: distribution resampling, label-space smoothing, representation-space calibration, and loss re-weighting. Distribution re-sampling methods directly modify the training data distribution by generating synthetic samples for rare label ranges. SMOGN [1] and SMOTEBoost-R [12] adapt popular synthetic oversampling techniques originally developed for classification tasks to continuous targets.

Label-space smoothing approaches adjust the label distribution or its granularity to alleviate the imbalance. LDS [25] smooths the empirical label density via Gaussian kernel convolution, enabling re-weighting schemes based on a more robust label distribution. HCA [23] constructs a hierarchy of discretized labels at varying granularities, using predictions from coarser levels to refine fine-grained predictions, balancing quantization errors and prediction accuracy.

Representation-space calibration tackles imbalance by enforcing structural regularities directly in latent feature space. FDS [25] aligns latent representations with smoothed label distributions. RankSim [6] explicitly calibrates the representation space to reflect the pairwise ranking structure in labels. ConR [9] introduces a contrastive regularizer that penalizes incorrect proximities in feature space based on label similarity and density, ensuring minority samples remain distinguishable. (For general regression, RnC [26] learns continuous, ranking-aware embeddings by contrasting samples based on their

relative ordering in label space. Ordinal Entropy [27] enforces local ordinal relationships via an entropy-based regularizer.)

Loss re-weighting (importance) methods rebalance the importance of each instance during training by adapting the regression objective. Inverse-frequency weighting is ubiquitous [25]; DenseLoss [20] employs label-density weighting calibrated linearly with a tunable parameter α . Balanced MSE [17] derives a closed-form objective assuming uniform label distributions, approximating the resulting integral numerically to address imbalance directly within the regression loss.

For imbalanced (long-tailed) classification, various approaches have been proposed, including resampling [29], logit adjustments [11], decoupled training [8], representation learning [7], uniform class separation [10], multiple branches [29], and multiple experts [28].

III. APPROACH

Preliminaries. Let $\{(x_i, y_i)\}_{i=1}^N$ be a training data set \mathcal{D} , where $x_i \in \mathbb{R}^d$ denotes the input of dimensionality d and $y_i \in \mathbb{R}$ is the label, which is a continuous target. We denote $z = g(x; \theta_g)$ as the latent representation for x , where $g(x; \theta_g)$ is the encoder parameterized by a neural network model with parameters θ_g . The final prediction \hat{y} is given by a regressor $f(z; \theta_f)$ that operates over z , where $f(\cdot; \theta_f)$ is parameterized by θ_f . Therefore, the prediction can be expressed as $\hat{y} = f(g(x; \theta_g); \theta_f)$.

Highly imbalanced distributions. We divide the targets into equal-width bins. We define the imbalanced frequency ratio as $\rho = freq_{max}/freq_{min}$, where $freq_{max}$ ($freq_{min}$) is the frequency of instances in the largest (smallest non-empty) bin. A distribution is *highly imbalanced* if $\rho \geq 1000$.

Estimating probability density distributions. We use Kernel Density Estimation (KDE) [19] with a Gaussian kernel. The estimated density $\hat{p}_Y(y)$ for target value y is: $\hat{p}_Y(y) = \frac{1}{Nh} \sum_j^K K((y - y_j)/h)$, where K is the kernel and h is the bandwidth. KDE is used in DenseLoss [20] and LDS [25].

We denote $\hat{d}_i = \hat{p}_Y(y_i)$. We normalize all densities into $(0, 1)$: $d_i = \hat{d}_i/(\hat{d}_{\max} + \epsilon)$, where \hat{d}_{\max} is the largest density and ϵ is a small constant (10^{-3}) so that $d_i \neq 1$ (and $MDI(d_i) \neq 0$ in Sec. III-A2). Henceforth d_i refers to the normalized density. We define the imbalance density ratio as $\rho_d = d_{\max}/d_{\min}$, where $d_{\max} = \max_i d_i$ ($d_{\min} = \min_i d_i$) is the maximum (minimum) normalized density. For KDE, bandwidth h is chosen such that the imbalance density ratio is close to the imbalance frequency ratio; that is, $\rho_d \approx \rho$.

To handle high imbalance, based on KDE, we use the MDI importance function (Sec. III-A) to shift importance away from frequent instances and toward rare instances. To consider correlation in addition to error, we use weighted Pearson Correlation Coefficient (wPCC, Sec. III-B) as a loss regularizer. Stratified Sampling (Sec. III-C) helps produce mini-batches that consistently contain rare samples. Our method is called CISIR, which uses wPCC with MDI in the loss function and stratified sampling for mini-batches (Algorithm 1).

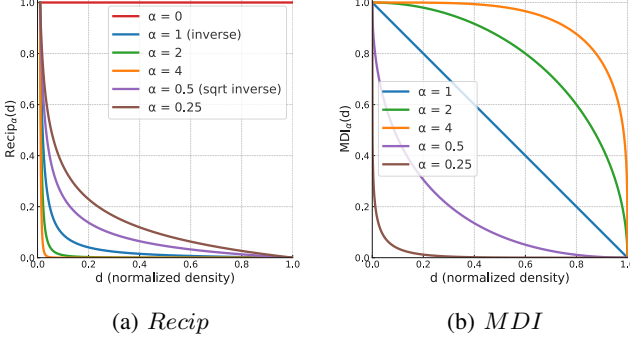


Fig. 2: *Recip* and *MDI* importance functions. For *Recip*, we rescale $r_i = \text{Recip}_\alpha(d_i)$ so that $r_i \in (0, 1]$ to match *MDI*.

A. Importance Functions

To encourage that both frequent and rare regions of the feature space are learned well, we attribute importance r_i to instance x_i with normalized density $d_i \in (0, 1)$ based on an *importance* (*Imp*) function:

$$r_i = \text{Imp}(d_i). \quad (1)$$

We use "importance" to distinguish it from a "weight" in the model. The importance function *Imp* is a monotonically decreasing function: the lower the normalized density d_i , the higher the resulting importance r_i . The importance can be precomputed once for a dataset and reused during training.

1) *Reciprocal Importance*: The inverse function [25] is a typical importance function due to its property of balancing the data distribution. To reduce the initial sharp decrease in importance at low density, square-root inverse [25] was also proposed. However, the desirable rate of initial decrease is generally not known and dependent on the dataset, imbalance ratio, and loss function.

To overcome these limitations, we generalize inverse and square-root inverse to a **Reciprocal importance** function that provides more flexibility in the rate of initial decrease in importance at low density. Given the normalized density d_i for instance x_i , we define the reciprocal importance (*Recip*) as:

$$\text{Recip}_\alpha(d_i) = \frac{1}{d_i^\alpha}, \quad \alpha \geq 0, \quad (2)$$

where α controls the curvature of the function:

- When $\alpha = 0$, the function reduces to a constant importance of 1 for all instances; ie, no adjustment for imbalance.
- When $\alpha = 1$, it is the typical inverse function $1/d_i$ that achieves the balanced distribution.
- When $\alpha > 1$, it further emphasizes the rare samples beyond the balanced distribution (which is beneficial to some datasets (Sec IV-C)).

Figure 2a shows Reciprocal importance with various α values.

2) *Monotonically Decreasing Involution (MDI) Importance*: Although Reciprocal importance provides an effective adjustment of importance among frequent and rare instances, it is

fundamentally limited by its inherent convexity and exponential form, restricting its ability to represent linear or concave importance relationships. Consequently, Reciprocal importance is insufficient when a more diverse range of importance shapes is needed in various imbalance scenarios.

To address these limitations, we introduce **Monotonically Decreasing Involution (MDI) importance**, a parameterized function with three properties: (1) it is monotonically decreasing, (2) it allows convex, linear, and concave functions to represent a diverse family of importance functions, and (3) it is an involution (or a self-inverse function, where $f(f(x)) = x$) to preserve the same property exhibited by the inverse function that yields a balanced distribution. Given a normalized density d_i for instance x_i , MDI importance is defined as:

$$\text{MDI}_\alpha(d_i) = (1 - d_i^\alpha)^{\frac{1}{\alpha}}, \quad \alpha > 0, \quad (3)$$

where α controls the curvature and shape of the function:

- When $0 < \alpha < 1$, the function is convex, similar to Reciprocal importance (Sec. III-A1).
- When $\alpha = 1$, it is linear, similar to DenseLoss [20].
- When $\alpha > 1$, it is concave (which is beneficial to some datasets (Sec IV-C)).
- When $\alpha \gg 1$, it is approximately 1 at low density.

Fig. 2b illustrates MDI importance with various α values.

B. Weighted Pearson Correlation Coefficient (wPCC) as Loss Regularization

For regression, as discussed in Sec. I, MSE does not differentiate models that are equally inaccurate but differ in correlation between the predicted and actual values. Also, while perfect MSE yields perfect positive correlation, perfect positive correlation does not guarantee perfect MSE. Hence, for imbalanced regression, we propose *wMSE* (weighted MSE) as the primary loss function and *wPCC* (weighted Pearson Correlation Coefficient) as the secondary loss function or regularization. Each instance i is weighted by importance r_i (Eq. 1), which has been normalized such that $\sum_{i=1}^N r_i = 1$. To allow different importance values (e.g. different α values in *MDI* for *wMSE* and *wPCC*) for the same instance in the two loss functions, we denote re_i and rc_i as the importance for instance i in *wMSE* and *wPCC* respectively. Moreover, re_i and rc_i are obtained from an importance function (*Recip* or *MDI* in Sec. III-A) with α values that we denote as α_e and α_c respectively.

We define *wMSE* as:

$$wMSE = \sum_{i=1}^N re_i (y_i - \hat{y}_i)^2, \quad (4)$$

and *wPCC* as:

$$wPCC = 1 - \frac{\sum_{i=1}^N rc_i (y_i - \bar{y})(\hat{y}_i - \bar{\hat{y}})}{\sqrt{\sum_{i=1}^N rc_i (y_i - \bar{y})^2} \sqrt{\sum_{i=1}^N rc_i (\hat{y}_i - \bar{\hat{y}})^2}}, \quad (5)$$

where \bar{y} and \hat{y} are the averages of y and \hat{y} respectively. Our proposed overall loss function is:

$$\mathcal{L} = wMSE + \lambda \cdot wPCC, \quad (6)$$

where $\lambda > 0$ adjusts the influence of $wPCC$.

Moreover, $wPCC$ can help reduce $wMSE$. Following the MSE decomposition in [13, Eq. 9], we have:

$$\begin{aligned} \text{MSE}(\hat{y}, y) &= (\bar{y} - \hat{y})^2 + \text{var}(\hat{y}) + \text{var}(y) \\ &\quad - 2 \cdot \text{cov}(\hat{y}, y), \end{aligned} \quad (7)$$

which, after some transformation, as shown in Appendix F, yields:

$$\begin{aligned} \text{MSE}(\hat{y}, y) &= (\bar{y} - \hat{y})^2 + (\text{sd}(\hat{y}) - \text{sd}(y))^2 \\ &\quad + 2 \cdot \text{sd}(\hat{y}) \cdot \text{sd}(y) (1 - \text{PCC}(\hat{y}, y)). \end{aligned} \quad (8)$$

where $\text{var}(\cdot)$, $\text{cov}(\cdot, \cdot)$, and $\text{sd}(\cdot)$ denote the variance, covariance, and standard deviation operators, respectively.

Eq. (8) is a sum of three terms: a term for mismatch in the mean, $(\bar{y} - \hat{y})^2$; a second term for mismatch in the standard deviation, $(\text{sd}(\hat{y}) - \text{sd}(y))^2$; and a third term, $2 \cdot \text{sd}(\hat{y}) \cdot \text{sd}(y) (1 - \text{PCC}(\hat{y}, y))$, related to the correlation deficit. While the first two terms encourage matching the moments of the data distribution, the third term's minimization highlights a critical point. MSE can be reduced by increasing the Pearson Correlation Coefficient, $\text{PCC}(\hat{y}, y)$, towards 1, and/or by decreasing the standard deviation of the predictions, $\text{sd}(\hat{y})$ towards 0.

In general, since the second term is present and $\text{sd}(y) \neq 0$, the prediction standard deviation $\text{sd}(\hat{y})$ does not collapse to zero. However, in some cases, illustrated by Model 1 (with no correlation) and Model 2 (with some correlation) in Fig. 1, MSE cannot distinguish the two models. This is caused by $\text{sd}(\hat{y})$ of Model 1 being zero, which renders the third term to be zero and the lack of correlation to be ignored. Similarly, a small $\text{sd}(\hat{y})$ diminishes the penalty due to poor correlation. To address this limitation, our proposed $wPCC$ regularizer directly penalizes poor correlation by minimizing $1 - \text{PCC}(\hat{y}, y)$.

C. Stratified Sampling in Mini-Batches (SSB)

Training neural networks with stochastic gradient descent (SGD) typically involves partitioning the dataset \mathcal{D} into mini-batches of size B , yielding $M = N/B$ mini-batches and parameter updates per epoch. With highly imbalanced data, uniformly sampled mini-batches may not represent rare target regions adequately. Consider the probability of rare samples as $\pi_r \approx 0$, the probability of no rare instances in a uniformly drawn mini-batch is $(1 - \pi_r)^B$, which is close to 1 when B is relatively small compared to $1/\pi_r$. That is, some mini-batches might not have rare instances at all, which lead to gradients that do not reduce loss for rare instances during some model updates.

To ensure rare instances are represented across mini-batches, we propose to perform stratified sampling to form mini-batches such that each mini-batch has a similar distribution as the overall training distribution. Consequently, gradients computed

Algorithm 1 CISIR Training Procedure

Require: Dataset \mathcal{D} , batch size B , hyperparameters $\alpha_e, \alpha_c, \lambda$, learning-rate η

- 1: Estimate densities d_i with KDE (Sec. III)
- 2: Compute importance re_i, rc_i using MDI (Eq. (3))
- 3: Form B groups with Stratified Sampling (Sec. III-C)
- 4: **while** model not converged **do**
- 5: Build mini-batch \mathcal{B} by drawing one sample from each group
- 6: Forward-propagate to obtain predictions \hat{y}_i
- 7: Compute $wMSE$ (Eq. (4)) and $wPCC$ (Eq. (5))
- 8: $\mathcal{L} \leftarrow wMSE + \lambda \cdot wPCC$ (Eq. (6))
- 9: Back-propagate $\nabla_{\theta} \mathcal{L}$ and update model parameters with step η
- 10: **end while**
- 11: **return** Trained model parameters θ

from these stratified mini-batches approximate the gradient computed over the training set, and every model update reduces loss for some rare instances.

To perform stratified sampling, we first choose M such that M is less than or equal to the number of rare instances. We sort all instances based on their target values. The sorted instances are then divided into B groups, each containing M instances (The final group may have fewer than M instances). The number of groups B matches the size of a mini-batch, with each group contributing one instance to the mini-batch. To create each mini-batch, we randomly select one instance from each of the B groups. For example, if larger target values are rarer, the M instances with the largest target values are in one group. Each of the M instances is randomly assigned to one of M mini-batches.

Algorithm 1 summarizes the overall CISIR method. We estimate densities via KDE on line 1. We then compute the importance values using MDI on line 2. With stratified sampling, we form B groups of data instances on line 3. From lines 4 to 9, we iteratively train the model by getting a mini-batch on line 5, taking the model's predictions on line 6, computing the loss with lines 7-8, and updating the model parameters on line 9. After convergence, the trained model is finally returned on line 11.

IV. EXPERIMENTAL EVALUATION

A. Datasets and Evaluation Metrics

We evaluate our method on five highly imbalanced datasets. SEP-EC aims to forecast the change (delta) in proton intensity based on features from electron intensity and CMEs (Coronal Mass Ejections). SEP-C focuses on forecasting peak proton intensity based on CMEs characteristics. SARCOS [22] estimates the torque vector based on joint-state inputs for a 7-DOF robot arm. Blog Feedback (BF) [3] forecasts the number of comments based on textual, temporal, and engagement features. Online News Popularity (ONP) [5] estimates the number of shares of an article based on content,

TABLE I: CISIR vs. recent methods (**bold** = best, underline = 2nd best, * = statistically significant)

Dataset	Method	MAE \downarrow	MAE $R \downarrow$	AORE \downarrow	PCC \uparrow	PCC $R \uparrow$	AORC \uparrow
SEP-EC	SQINV+LDS+FDS	0.177	<u>0.566</u> *	0.371	-0.025	0.067	0.021
	BalancedMSE	0.161	0.659	0.410	-0.036	0.141	0.053
	DenseLoss	0.071 *	0.626	<u>0.348</u> *	0.286	<u>0.699</u> *	0.493
	Recip+wPCC+SSB	<u>0.089</u> *	0.606	<u>0.348</u> *	0.219	<u>0.699</u> *	0.459
	CISIR	0.184	0.441 *	0.313 *	<u>0.274</u> *	0.703	<u>0.488</u> *
SEP-C	SQINV+LDS+FDS	1.681	4.314	2.997	0.173	0.481	0.327
	BalancedMSE	1.683	3.614	2.649	0.394	0.393	0.393
	DenseLoss	0.237 *	2.245	<u>1.241</u>	<u>0.690</u> *	0.588	0.639
	Recip+wPCC+SSB	1.173	1.376 *	1.274	0.627	0.661 *	<u>0.644</u>
	CISIR	<u>0.335</u> *	<u>1.875</u> *	1.105 *	0.702	0.593	0.647
SARCOS	SQINV+LDS+FDS	0.575	0.748	0.661	0.020	-0.049	-0.015
	BalancedMSE	0.571	1.694	1.132	0.189	-0.170	0.010
	DenseLoss	0.058	0.076	0.067	0.964	0.830	0.897
	Recip+wPCC+SSB	0.053	<u>0.071</u>	0.062	0.986	0.910 *	0.948 *
	CISIR	<u>0.055</u>	0.069	0.062	<u>0.982</u> *	0.876*	0.929*
BF	SQINV+LDS+FDS	1.036	1.780	1.408	-0.152	0.065	-0.044
	BalancedMSE	0.689	1.769	1.229	-0.011	0.066	0.028
	DenseLoss	0.169 *	0.747	0.458	<u>0.735</u>	0.301	0.518
	Recip+wPCC+SSB	<u>0.187</u> *	<u>0.740</u>	<u>0.463</u> *	0.733	<u>0.319</u> *	0.526
	CISIR	0.280	0.709 *	0.495	0.737	<u>0.330</u> *	0.533
ONP	SQINV+LDS+FDS	2.628	4.438	3.533	0.034	-0.012	0.011
	BalancedMSE	2.798	4.154	3.476	-0.028	0.012	0.047
	DenseLoss	0.317	<u>1.311</u>	<u>0.814</u>	0.325 *	0.054	0.189
	Recip+wPCC+SSB	<u>0.326</u>	1.351	0.838	0.288	0.095	<u>0.192</u>
	CISIR	0.379	1.180 *	0.780	<u>0.299</u> *	<u>0.093</u> *	0.196

TABLE II: Incorporating wPCC into other methods (**bold** = best, * = statistically significant)

Method	SEP-EC		SEP-C		SARCOS		BF		ONP	
	AORE \downarrow	AORC \uparrow								
SQINV+LDS+FDS	0.371	0.021	2.997	0.327	0.661	-0.015	1.408	-0.044	3.533	0.011
+ wPCC	0.371	0.270 *	2.891	0.411 *	0.657	0.051 *	1.062 *	0.130 *	3.416 *	0.038
BalancedMSE	0.410	0.053	2.649	0.393	1.132	0.010	1.229	0.028	3.476	0.047
+ wPCC	0.392	0.057	2.484	0.491 *	0.884 *	0.097 *	0.990	0.162 *	3.223 *	0.086 *
DenseLoss	0.348	0.493	1.241	0.639	0.067	0.897	0.458	0.518	0.814	0.189
+ wPCC	0.344	0.500	1.084	0.660	0.062	0.920 *	0.458	0.529	0.791	0.203

topic, and sentiment attributes. Each dataset's imbalance ratio (ρ) is in Table III. SARCOS, BF, and ONP datasets are available at [2], [4], [21]. Our SEP datasets are available in <https://huggingface.co/datasets/Machine-Earning/CISIR-datasets/resolve/main/CISIR-data.zip>.

Our evaluation metrics on the test set include overall *MAE* (Mean Absolute Error) and *PCC* (Pearson Correlation Coefficient). *MAE_R* (*PCC_R*) denotes *MAE* (*PCC*) of rare instances that are important. For SEP-EC, only positive (increasing intensity) rare instances are included in *MAE_R* and *PCC_R*. Since we would like to consider all instances with an emphasis on rare instances, we propose two hybrid metrics. We define the average of overall and rare *MAE* as: *AORE* = (*MAE* + *MAE_R*) / 2, and overall and rare *PCC* as:

AORC = (*PCC* + *PCC_R*) / 2. *AORE* and *AORC* are our main evaluation metrics, with *AORE* being more important than *AORC* (as we discussed in Sec.I that error is more important than correlation). To determine if two averages of measurements are different with statistical significance, we use standard error.

B. Baseline Methods and Experimental Procedures

Since our proposed CISIR is most similar to DenseLoss [20], LDS/FDS [25], and Balanced MSE [17], they are the baseline methods. We do not include methods that need substantive additional computation due to factors such as additional synthetic instances and separate representation learning. For LDS/FDS, we choose SQINV+LDS+FDS, which is the more

TABLE III: Comparison of importance functions (**bold** = best, underline = 2nd best, * = statistically significant)

Importance functions	AORE↓				
	SEP-C	SARCOS	ONP	SEP-EC	BF
Imb. ratio ρ	1,476	3,267	6,746	10,478	33,559
INV	2.456	0.064	0.849	0.362	0.451
SQINV	1.313	0.068	<u>0.765</u>	0.369	<u>0.447</u>
DenseLoss	<u>1.277</u>	0.065	0.842	0.355	0.471
Recip	1.289	<u>0.063</u>	0.764	<u>0.349</u>	0.445
MDI	1.105*	0.062	0.780	0.313*	0.495
α_e in Recip	0.70	1.10	0.90	1.20	0.70
α_e in MDI	2.40	0.20	1.10	0.01	0.50

TABLE IV: Ablation study of CISIR on the SEP-EC dataset (**bold** = best, underline = 2nd best)

Method	AORE↓		AORC↑
CISIR	0.313		0.488
w/o MDI (with INV)	0.362 (+0.049)		0.447 (-0.041)
w/o wPCC	1.160 (+ 0.847)		0.194 (- 0.294)
w/o SSB	0.333 (+0.020)		0.463 (-0.025)

effective variant [25]. Also, we include a variant of CISIR denoted as Recip+wPCC+SSB, which uses Recip instead of MDI. The baseline results are obtained by implementing DenseLoss ourselves, while using the authors’ implementations, including their hyperparameters, of LDS/FDS [24] and Balanced-MSE [16]. Our source code is available in <https://github.com/Machine-Earning/CISIR>.

All experiments are implemented in TensorFlow 2.6 and executed on NVIDIA RTX 2080Ti (11GB), A100 (40GB), and H100 (80GB) GPUs. Each experiment is repeated with five fixed seeds; reported results are averages over these runs. For all datasets, we use a residual MLP architecture with LeakyReLU activations, batch normalization, with dataset-specific hidden units, embedding dimensions, dropout rates, weight-decay values, batch sizes, and initial learning rates. Models are trained till convergence with Adam optimizer, early stopping based on validation loss, and a learning-rate scheduler reducing by a factor of 0.95 after 50 stagnant epochs. If training and testing subsets are provided, we use them directly; otherwise, we adopt a 2/3–1/3 split for training and testing with stratified sampling, performing four-fold cross-validation on the training portion, again with stratified sampling.

C. Results

Table I has our main results in comparing CISIR to other recent methods. We observe that CISIR achieves the lowest AORE in 4 datasets, while it achieves the highest AORC in 3 and the second highest in the remaining 2 datasets. That is, generally, CISIR outperforms the other methods based on our main evaluation metrics. Focusing on important rare instances, CISIR has the lowest MAE_R in 4 and the second lowest in the remaining dataset. While CISIR has the highest PCC_R

in 2 datasets, Recip+wPCC+SSB (a variant of CISIR) has the highest in 3 datasets. That is, CISIR and its variant generally outperform the other methods on rare instances.

Incorporating wPCC into other methods. To evaluate how wPCC can benefit other methods, we incorporate it into other methods. According to Table II, wPCC mostly improves all 3 methods across all 5 datasets in both AORE and AORC. The only exceptions are SQINV+LDS+FDS on SEP-EC and DenseLoss on BF, where AORC improved while AORE did not change. That is, generally, wPCC can improve the performance of other methods. This indicates that the constraint from wPCC in the loss not only improves correlation, but also reduces error.

Comparing importance functions. To compare importance functions directly, we use and fix wPCC (Eq. 5) and SSB (Sec. III-C), but only vary importance functions for wMSE (Eq. 4). INV is the inverse and SQINV is the square-root inverse [25]. Table III shows the AORE results. Since we fix wPCC, AORC is not directly affected and is not included in the table. MDI achieves the lowest AORE in 3 datasets and Recip in 2 datasets. That is, MDI generally outperforms the other importance functions.

To analyze if the imbalance ratio (ρ) of a dataset is related to α in Recip (Eq. 2) or MDI (Eq. 3), we include ρ and α_e (which is used to obtain importance re_i for wMSE in Eq. 4) in Table III. However, we do not observe a meaningful relationship between ρ and α_e . Unlike the other importance functions, we design MDI to include concave functions when $\alpha > 1$ (Eq. 3). From Table III, we observe that the SEP-C and ONP datasets benefit from concave functions with $\alpha_e > 1$. Also, we design Recip to allow further emphasis on rare instances beyond the balanced distribution when $\alpha > 1$ (Eq. 2). We observe that the SARCOS and SEP-EC datasets benefit from further emphasis on rare instances with $\alpha_e > 1$.

Based on the observations above, the weaker performance of SQINV+LDS+FDS and Balanced MSE in Table I may be due to the absence of wPCC, which can reduce error and increase correlation. Also, SQINV is equivalent to Recip with $\alpha = 0.5$, but α_e for Recip in Table III can be quite different. Our datasets are highly imbalanced, but their datasets might not be (imbalance ratios were not usually reported). While LDS uses KDE, it does not explicitly maintain the imbalance ratio ($\rho_d \approx \rho$) in KDE (Sec.III), which might be important for high imbalance ratios.

D. Analyses

To further analyze the main results on the SARCOS dataset, we plot the actual vs. predicted values in Figure 3. Rare instances are in the top right and bottom left corners. Both SQINV+LDS+FDS and Balanced MSE have more difficulty with rare instances than the other 3 methods, which perform similarly. Focusing on the the top right corner, Recip+wPCC+SSB is more accurate. However, focusing on the few rarest instances on the far top right corner, CISIR is more accurate. Focusing on the bottom left corner, CISIR is more accurate.

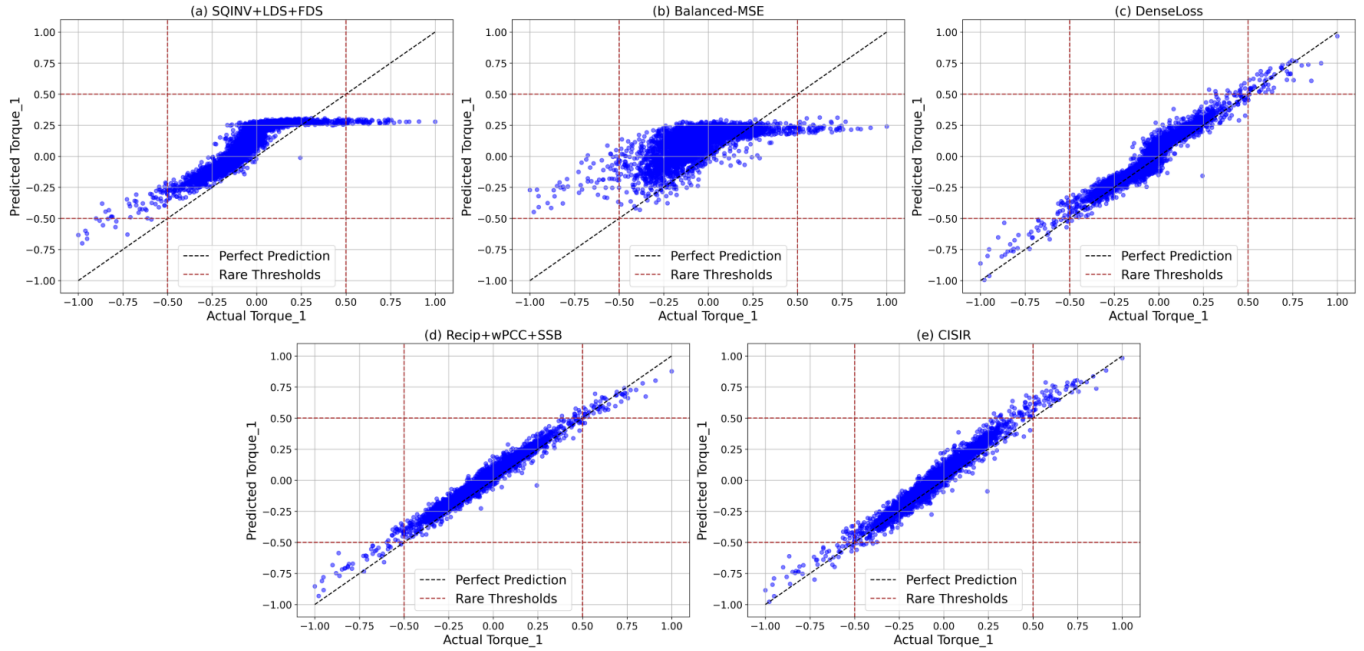


Fig. 3: Actual vs. predicted values on the SARCOS dataset.

TABLE V: Effects of $wPCC$ on CISIR’s MSE decomposition terms for SEP-EC. CISIR- $wPCC$ denotes CISIR without $wPCC$.

Test Subset	$(\bar{y} - \hat{y})^2$			$(\text{sd}(\hat{y}) - \text{sd}(y))^2$			$2 \text{sd}(\hat{y}) \text{sd}(y) (1 - \text{PCC}(\hat{y}, y))$			$1 - \text{PCC}(\hat{y}, y)$		
	CISIR-wPCC	CISIR	% Δ	CISIR-wPCC	CISIR	% Δ	CISIR-wPCC	CISIR	% Δ	CISIR-wPCC	CISIR	% Δ
All	0.145	0.024	-83.3	1.199	0.000	-100.0	0.304	0.025	-91.6	0.963	0.726	-24.5
Rare	0.366	0.149	-59.2	0.786	0.027	-96.5	0.367	0.061	-83.3	0.649	0.297	-54.3

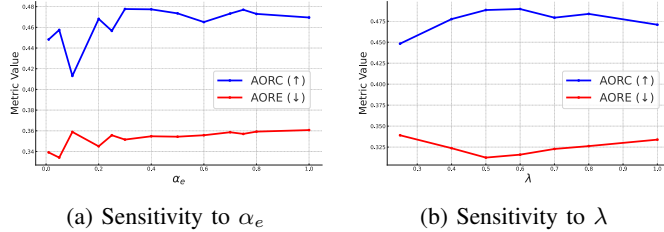


Fig. 4: Sensitivity analysis of CISIR to α_e and λ on SEP-EC.

Ablation study. Results from an ablation study on CISIR with the SEP-EC dataset are in Table IV. We observe that each of the 3 proposed components (MDI, $wPCC$, and SSB) contributes to CISIR. Particularly, $wPCC$ contributes the most. Moreover, $wPCC$ not only increases correlation (AORC), it also reduces error (AORE). This indicates that the constraint from $wPCC$ in the loss helps achieve a lower local minimum for wMSE during training.

Three components of MSE decomposition.

Following Eq. (8), MSE decomposes into three terms: the first term $(\bar{y} - \hat{y})^2$ captures mean mismatch, the second term $(\text{sd}(\hat{y}) - \text{sd}(y))^2$ captures standard deviation mismatch, and the third term $2 \text{sd}(\hat{y}) \text{sd}(y) (1 - \text{PCC}(\hat{y}, y))$ captures correlation

deficit. We analyze how including $wPCC$ regularization affects these three components on the SEP-EC dataset. Since $wPCC$ directly optimizes correlation by minimizing $1 - \text{PCC}(\hat{y}, y)$, we expect it to primarily reduce the third term. Table V shows the decomposition results for CISIR with and without $wPCC$ on both the full test set (*All*) and rare events (*Rare*). Also, $1 - \text{PCC}$ is shown separately in the last column. As expected, $1 - \text{PCC}$ and the third term are reduced. However, the first two terms are also reduced.

Without $wPCC$, the second term is the largest contributor to total MSE (1.199 for *All*, 0.786 for *Rare*), dominating both the first term (0.145 and 0.366) and third term (0.304 and 0.367). Including $wPCC$ produces reductions across all three components: -83.3% (first term), -100.0% (second term), and -91.6% (third term) for the full test set, and similarly for rare events (-59.2% , -96.5% , and -83.3% respectively). The near-complete elimination of the second term is particularly notable, reducing from 1.199 to 0.000 for all samples and from 0.786 to 0.027 for rare events. This suggests that $wPCC$ regularization constrains the model to produce predictions with variability matching the true distribution, addressing the issues inherent in MSE-only optimization.

The third term reductions (-91.6% for *All*, -83.3% for

Rare), directly reflect the intended effect of $wPCC$ on correlation. To isolate the pure correlation improvement from the standard deviation weighting in the third term, we additionally report $1 - \text{PCC}(\hat{y}, y)$ as a correlation degradation metric. The $wPCC$ regularizer reduces correlation degradation by -24.5% for all samples (from 0.963 to 0.726, corresponding to PCC improving from 0.037 to 0.274) and by -54.3% for rare events (from 0.649 to 0.297, corresponding to PCC improving from 0.351 to 0.703). The stronger improvement for rare events demonstrates that $wPCC$ is effective at maintaining correlation where it matters most.

The first term, while showing the smallest absolute values, still improves by -83.3% for the full test set, and by -59.2% for the rare event subset. Overall, the decomposition reveals that $wPCC$ addresses multiple aspects of prediction quality simultaneously, with its most pronounced effect being the correction of prediction standard deviation mismatch (second term), followed by improved correlation (third term and $1 - \text{PCC}$) and reduced bias (first term).

Parameter Sensitivity. In CISIR, α_e (α_c) is used to vary the MDI importance function (Eq. 3), which in turn varies the importance to instances in wMSE ($wPCC$). λ varies the contribution of $wPCC$ to the overall loss (Eq.6).

From Figure 4a, we observe that AORE generally degrades, while AORC generally improves, when α_e increases. That is, AORE and AORC are trading off when α_e varies. Since α_e affects wMSE (which affects AORE), we prefer $\alpha_e < 0.1$ (which indicates large importance from rare instances).

From Sec. III-B, α_c governs the importance rc_i . Empirically, $rc_i = 1$ (*i.e.*, not using MDI and assigning equal importance to every instance) already enables $wPCC$, together with an appropriately chosen λ , to lower error and raise correlation in almost all scenarios. Across the five datasets, only SEP-C needed α_c to be set to 1.7 (which is another example where an "atypical" concave function is beneficial).

From Figure 4b, we observe that AORE bottoms and AORC peaks when λ is in the range of $0.5 - 0.6$. We note that AORE and AORC generally improve and degrade together. That is, AORE and AORC are not trading off and can be optimized together by varying λ . Also, this provides further evidence that $wPCC$ (controlled by λ) is beneficial in not only increasing correlation, but also reducing error.

V. CONCLUSION, LIMITATIONS, AND BROADER IMPACTS

For highly imbalanced regression with tabular data, we propose CISIR that incorporates $wPCC$ as a secondary loss function, MDI importance that allows convex, linear, and concave functions, and stratified sampling in the mini-batches. Our experimental results indicate that CISIR can achieve lower error and higher correlation than some recent methods. Also, adding our $wPCC$ component to other methods is beneficial in not only improving correlation, but also reducing error. Lastly, MDI importance can outperform other importance functions.

While MDI importance allows a linear function, it does not allow the slope to vary (which involves another parameter) as DenseLoss [20] does. The claims of this study are limited to

the included methods and datasets. While our proposed $wPCC$ component is for imbalanced regression, our rationale in Sec. I is for general regression, so $wPCC$ can benefit regression in general. Our proposed CISIR can benefit other applications; *e.g.*, estimating rare large credit card fraudulent transactions and rare severe outcomes of diseases. We do not anticipate negative societal impacts.

REFERENCES

- [1] Paula Branco, Luís Torgo, and Rita P Ribeiro. Smogn: a pre-processing approach for imbalanced regression. In *First international workshop on learning with imbalanced domains: Theory and applications*, 2017.
- [2] Krisztian Buza. Blogfeedback data set, 2014. <https://archive.ics.uci.edu/dataset/304/blogfeedback>.
- [3] Krisztian Buza. Feedback prediction for blogs. In *Data Analysis, Machine Learning and Knowledge Discovery, Studies in Classification, Data Analysis, and Knowledge Organization*, pages 145–152. Springer, Cham, 2014.
- [4] Kelwin Fernandes. Online news popularity data set, 2015. <https://archive.ics.uci.edu/dataset/332/online+news+popularity>.
- [5] Kelwin Fernandes, Pedro Vinagre, and Paulo Cortez. A proactive intelligent decision support system for predicting the popularity of online news. In *Proceedings of the 17th Portuguese Conference on Artificial Intelligence (EPIA 2015), Progress in Artificial Intelligence*, volume 9273 of *Lecture Notes in Computer Science*, pages 535–546. Springer, 2015.
- [6] Yu Gong, Greg Mori, and Fred Tung. Ranksim: Ranking similarity regularization for deep imbalanced regression. In *International Conference on Machine Learning*, 2022.
- [7] Bingyi Kang, Yu Li, Sa Xie, Zehuan Yuan, and Jiashi Feng. Exploring balanced feature spaces for representation learning. In *International Conference on Learning Representations*, 2021.
- [8] Bingyi Kang, Saining Xie, Marcus Rohrbach, Zhicheng Yan, Albert Gordo, Jiashi Feng, and Yannis Kalantidis. Decoupling representation and classifier for long-tailed recognition. In *International Conference on Learning Representations*, 2020.
- [9] Mahsa Keramati, Lili Meng, and R David Evans. Conr: Contrastive regularizer for deep imbalanced regression. In *International Conference on Learning Representations*, 2024.
- [10] Tianhong Li, Peng Cao, Yuan Yuan, Lijie Fan, Yuzhe Yang, Rogerio S Feris, Piotr Indyk, and Dina Katabi. Targeted supervised contrastive learning for long-tailed recognition. In *Proceedings of the IEEE/CVF conference on computer vision and pattern recognition*, pages 6918–6928, 2022.
- [11] Aditya Krishna Menon, Sadeep Jayasumana, Ankit Singh Rawat, Himanshu Jain, Andreas Veit, and Sanjiv Kumar. Long-tail learning via logit adjustment. In *International Conference on Learning Representations*, 2021.
- [12] Nuno Moniz, Rita Ribeiro, Vitor Cerqueira, and Nitesh Chawla. Smote-boost for regression: Improving the prediction of extreme values. In *2018 IEEE 5th international conference on data science and advanced analytics (DSAA)*, 2018.
- [13] Allan H Murphy. Skill scores based on the mean square error and their relationships to the correlation coefficient. *Monthly weather review*, 116(12):2417–2424, 1988.
- [14] Arik Posner. Up to 1-hour forecasting of radiation hazards from solar energetic ion events with relativistic electrons. *Space Weather*, 5(5), 2007.
- [15] Donald V Reames. *Solar energetic particles: a modern primer on understanding sources, acceleration and propagation*. Springer Nature, 2021.
- [16] Jiawei Ren. Balanced mse for imbalanced regression, 2022. GitHub repository: <https://github.com/jiawei-ren/BalancedMSE>.
- [17] Jiawei Ren, Mingyuan Zhang, Cunjun Yu, and Ziwei Liu. Balanced mse for imbalanced visual regression. In *Proceedings of the IEEE/CVF Conference on Computer Vision and Pattern Recognition*, 2022.
- [18] IG Richardson, ML Mays, and BJ Thompson. Prediction of solar energetic particle event peak proton intensity using a simple algorithm based on cme speed and direction and observations of associated solar phenomena. *Space Weather*, 2018.
- [19] Bernard W Silverman. *Density estimation for statistics and data analysis*. Routledge, 2018.

[20] Michael Steininger, Konstantin Kobs, Padraig Davidson, Anna Krause, and Andreas Hotho. Density-based weighting for imbalanced regression. *Machine Learning Journal*, 2021.

[21] Sethu Vijayakumar. Gaussian processes for machine learning - sarcos dataset, 2000. <http://www.gaussianprocess.org/gpml/data/>.

[22] Sethu Vijayakumar and Stefan Schaal. SARCOS robot-arm inverse dynamics dataset. Supplementary material to “LWPR: An $O(n)$ Algorithm for Incremental Real-Time Learning in High-Dimensional Space”, 2000.

[23] Haipeng Xiong and Angela Yao. Deep imbalanced regression via hierarchical classification adjustment. In *Proceedings of the IEEE/CVF Conference on Computer Vision and Pattern Recognition*, 2024.

[24] Yuzhe Yang. Delving deeper in imbalanced regression (lds/fds), 2021. GitHub repository: <https://github.com/YyzHarry/imbalanced-regression>.

[25] Yuzhe Yang, Kaiwen Zha, Yingcong Chen, Hao Wang, and Dina Katabi. Delving into deep imbalanced regression. In *International Conference on Machine Learning*, 2021.

[26] Kaiwen Zha, Peng Cao, Jeany Son, Yuzhe Yang, and Dina Katabi. Rank-n-contrast: Learning continuous representations for regression. *Advances in Neural Information Processing Systems*, 2023.

[27] Shihao Zhang, Linlin Yang, Michael Bi Mi, Xiaoxu Zheng, and Angela Yao. Improving deep regression with ordinal entropy. In *The Eleventh International Conference on Learning Representations*, 2022.

[28] Yifan Zhang, Bryan Hooi, Lanqing Hong, and Jiashi Feng. Self-supervised aggregation of diverse experts for test-agnostic long-tailed recognition. *Advances in neural information processing systems*, 35:34077–34090, 2022.

[29] Boyan Zhou, Quan Cui, Xiu-Shen Wei, and Zhao-Min Chen. Bbn: Bilateral-branch network with cumulative learning for long-tailed visual recognition. In *Proceedings of the IEEE/CVF conference on computer vision and pattern recognition*, 2020.

APPENDIX

A. Involution in MDI influence

The following shows that MDI influence in Eq. 3 is an involution. Let $r_i = \text{MDI}_\alpha(d_i)$:

$$\begin{aligned} r_i &= (1 - d_i^\alpha)^{\frac{1}{\alpha}} \\ r_i^\alpha &= 1 - d_i^\alpha \\ d_i^\alpha &= 1 - r_i^\alpha \\ d_i &= (1 - r_i^\alpha)^{\frac{1}{\alpha}} \end{aligned} \quad (9)$$

B. Details of datasets

Further details of the five datasets are in Table VI.

TABLE VI: Dataset statistics and bin composition (sorted by imbalance ratio ρ)

Dataset	Imb. ρ	Lower Thr.	Upper Thr.	% Bin 1	% Bin 2	% Bin 3
SEP-C	1,476	–	ln(10)	98.04	–	1.96
SARCOS	3,267	–0.5	0.5	2.77	89.03	8.20
ONP	6,746	log(350)	log(35k)	0.81	98.30	0.89
SEP-EC	10,478	–0.5	0.5	0.77	98.09	1.14
BF	33,559	log(4)	log(40)	80.81	15.86	3.33

C. Architecture and training hyperparameters

For each dataset, the MLP architecture is in Table VII and the hyperparameters are in Table VIII.

D. Tuning hyperparameters α_e , α_c , and λ

In practice, we tune the three hyperparameters sequentially. We first fix $\lambda = 0.5$ to start with, giving wPCC its default secondary role in the loss, and vary α_e to ensure adequate rare influence through wMSE. Then, keeping this α_e fixed, we

TABLE VII: Dataset-specific MLP architecture

Dataset	Hidden-layer widths	Embed dim	Dropout
BF	4096–512–2048–512–1024–512	512	0.10
ONP	2048–128–1024–128–512–256–128	128	0.10
SARCOS	512–32–256–32–128–32–64–32	32	0.20
SEP-C	512–32–256–32–128–32–64–32	32	0.50
SEP-EC	2048–128–1024–128–512–128–256–128	128	0.20

TABLE VIII: Training hyperparameters

Dataset	Batch size	Init. LR	W. decay	ES patience	Bandw.
BF	4 096	1×10^{-4}	0.01	3 000	0.552
ONP	16 384	5×10^{-4}	0.10	3 000	1.429
SARCOS	14 800	5×10^{-4}	0.10	3 000	1.508
SEP-C	200	5×10^{-4}	1.00	3 000	0.880
SEP-EC	2 400	1×10^{-4}	0.10	4 000	0.070

vary λ to jointly lower error and raise correlation. Only if the correlation on rare instances remains unsatisfactory do we set and vary α_c to give more influence to rare instances in wPCC.

E. Weaker performance of SQINV+LDS+FDS and Balanced MSE

Our datasets are tabular, their datasets usually contain images. We use the authors’ implementations as well as their hyperparameters. While their hyperparameters are effective for their datasets, they might not be as effective in our datasets.

F. MSE decomposition

$$\text{MSE}(\hat{y}, y) = (\bar{y} - \bar{\hat{y}})^2 + \text{var}(\hat{y}) + \text{var}(y) - 2 \text{cov}(\hat{y}, y) \quad (1)$$

$$\begin{aligned} &= (\bar{y} - \bar{\hat{y}})^2 + (\text{var}(\hat{y}) + \text{var}(y) - 2 \text{sd}(\hat{y}) \text{sd}(y)) \\ &\quad + 2 \text{sd}(\hat{y}) \text{sd}(y) - 2 \text{cov}(\hat{y}, y) \end{aligned} \quad (2)$$

$$\begin{aligned} &= (\bar{y} - \bar{\hat{y}})^2 + (\text{sd}(\hat{y}) - \text{sd}(y))^2 \\ &\quad + 2(\text{sd}(\hat{y}) \text{sd}(y) - \text{cov}(\hat{y}, y)) \end{aligned} \quad (3)$$

$$\begin{aligned} \text{MSE}(\hat{y}, y) &= (\bar{y} - \bar{\hat{y}})^2 + (\text{sd}(\hat{y}) - \text{sd}(y))^2 \\ &\quad + 2 \text{sd}(\hat{y}) \text{sd}(y) (1 - \text{PCC}(\hat{y}, y)). \end{aligned} \quad (4)$$